

Developing brittle transparent materials with 3D fractures and experimental study

Jing Wang^{*}, Shucaï Li^a, Weishen Zhu^b and Liping Li^c

*Geotechnical and Structural Engineering Research Center, Shandong University,
No. 17923, Jingshi Road, Jinan, 250061, P.R. China*

(Received December 04, 2015, Revised October 12, 2016, Accepted October 13, 2016)

Abstract. The fracture propagation mechanism and fractured rock mass failure mechanism were important research in geotechnical engineering field. Many failures and instability in geotechnical engineering were related on fractures propagation, coalescence and interaction in rock mass under the external force. Most of the current research were limited to two-dimensional for the brittleness and transparency of three-dimensional fracture materials couldn't meet the requirements of the experiment. New materials with good transparent and brittleness were developed by authors. The making method of multi fracture specimens were established and made molds that could be reused. The tension-compression ratio of the material reached above 1/6 in normal temperature. Uniaxial and biaxial loading tests of single and double fracture specimens were carried out. Four new fractures were not found in the experiment of two-dimensional fractures such as the fin shaped crack, wrapping wing crack and petal crack and anti-wing crack. The relationship between stress and strain of the specimens were studied. The specimens with the load had experienced four stages of deformation and the process of the fracture propagation was clearly seen in each stage. The expansion characteristics of the fractured specimens were more obvious than the previous research.

Keywords: rock with fractures; transparent and brittle material; prefabricating crack; 3D crack extending; failure law

1. Introduction

There are lots of fractures in rock mass. These fractures are the weak parts of the surrounding rock under the condition of tunnel excavation and operation. The propagation and coalescence of the fractures could cause the rock mass failure and engineering instability. So it's an important subject to study the fracture process and fracture mechanism under the condition of stress in rock mass. First, fractures propagation tests under uniaxial or multi axial stress were carried out. Then combined with numerical methods, the corresponding mechanical model was established to reveal

*Corresponding author, Ph.D., E-mail: wjingsdu@163.com

^a Professor, E-mail: lishucaï@sdu.edu.cn

^b Professor, E-mail: zhuweishen@sdu.edu.cn

^c Professor, E-mail: yuliyangfan@163.com

the deformation, strength characteristics and failure mechanism of the rock mass. It was a necessary research approach. (Morozov and Petrov 2013, Zhang and Zhao 2013, Beygi 2013).

At present, most previous studies focused on the two-dimensional fractures. Such as Wang (2014), Scholtès and Donzé (2012) and Cheng (2014) studied initiation, propagation and coalescence mechanism of a single or multiple group of open crack with a prefabricated opening under uniaxial compression through experiment and numerical method. Some regularity of crack propagation were revealed and applied to the engineering practice. Sahouryeh *et al.* (2002) carried out the model test of similar materials and simulated the propagation of crack under biaxial conditions. Single and three - axis test of sandstone and gypsum model with different spacing and direction through joints were carried out by Ramamurthy (2001). Tang (2005) studied the expansion mechanism of prefabricated cracks in sandstone material and real rock sample. Then the numerical simulation and theoretical study of the rock bridges strength and fracture coalescence were made out. Cetisli and Kaman (2014) and Luo *et al.* (2012) studied the crack problem in composite plates jointed with composite patch by using numerical and experimental analysis. But two dimensional fracture model usually couldn't reflect the reality of the three dimensional, simplification of 3D fracture into two-dimensional crack would lose many important 3D information. So how to prepare the specimen with three dimensional fracture was a key problem. There were four forms of new fracture morphology under three dimensional fracture conditions, such as the fin shaped crack, wrapping wing crack and petal crack and anti-wing crack. They were not appeared in the case of two-dimensional crack.

Many scholars have done a lot of research 3D crack propagation. But the specimens containing three-dimensional fractures was very difficult to make. Because it not only need to ensure a certain tension and compression ratio, but also to ensure the transparency for observing the fracture propagation process. Tang (2015) and Mostafavi (2013) studied the crack growth of three dimensional crack under different loading conditions by using the organic glass, CR-39 resin and so on. But the plasticity of the resin they adopted was too large and the brittleness was too low. The ratio of tensile and compressive strength could only reach 1/3-1/5 under low temperature condition (-17 degrees C), which was far from the brittleness degree of the rock material. Shandong University scholars have found the transparent unsaturated polyester resin which ratio of tensile and compressive strength could reach 1/5 in low temperature conditions (-20 degrees Celsius). The brittleness degree was improved. But that test temperature conditions were difficult to achieve in the general laboratory. The plastic deformation easily occurred in the experiment, so the accuracy of experimental results was affected.

After several years study, we first made the similar materials which tensile strength to compressive strength ratio could reach more than 6:1 in the condition of normal temperature. Based on the excellent transparency, the initiation and propagation process of multiple cracks in the specimen could be observed throughout the whole experiment. The fracture mechanism and strength characteristics of several three-dimensional fracture specimens under uniaxial and biaxial conditions were studied. The technology and method of multi-fracture were developed, such as vacuum treatment of the mixed resin which increased the transparency. The prior fracture plate was changed from the prior metal sheet to the mica plate, so the weak surface was more real. The molds were made for easy disassembly and recycling. The materials developed in this paper made up for the shortcomings of previous studies. It was considered to an important new development in the field of research in recent years. This research had great significance for the future experimental research, theoretical analysis and engineering application.

2. Material preparation and experimental design of a three dimensional fracture resin

2.1 Brittle transparent resin material

In order to simulate the mechanical properties of the material, it was necessary to ensure that the material's main characteristics were close to the brittle rock, and the specimens' size met the required of the fractures. The specimens were mainly made of resin, curing agent, accelerator and other materials according to a certain proportion of mixing. Temperature and different mixture ratios were two important factors which influenced the mechanical properties of the materials in the process of resin molding.

In this paper, the mechanical properties of materials under different temperature and ratio conditions were studied based on a large number of experiments. At last, a brittle modified resin was obtained. Now there were two different experimental schemes which all included the good materials and formulations for the test. Scheme one contained A and B unsaturated resin and scheme two contained C epoxy resin. All of them could be produced with two-dimensional or three-dimensional fractures in the block test. The raw materials were shown in Figs. 1 and 2.

A was general benzene type unsaturated resin, with moderate viscosity and moderate reaction activity. The appearance was a transparent dark brown liquid, suitable for manufacture of glass fiber reinforced plastic and molded products. B was also general benzene type unsaturated resin,

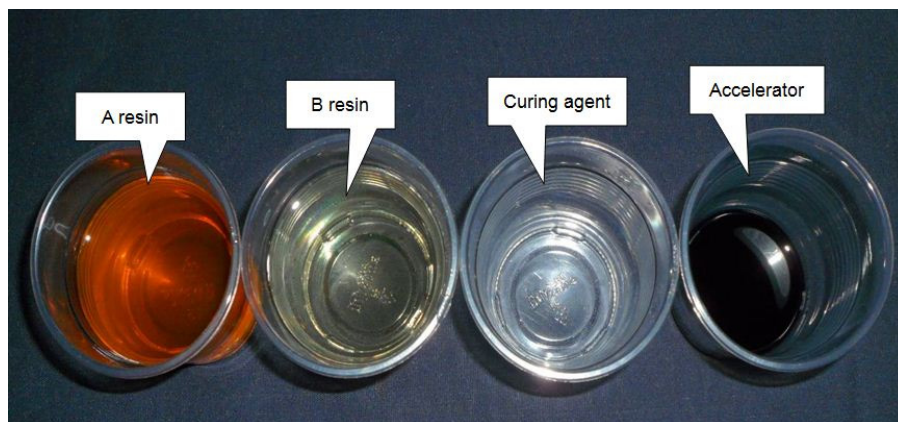


Fig. 1 Unsaturated resin and burden used to configurate similar materials (scheme one)

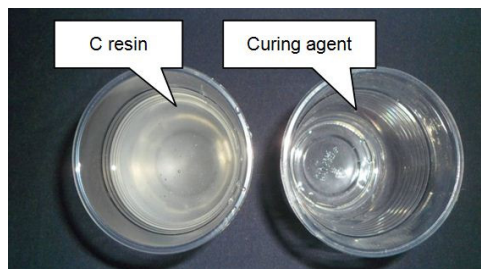


Fig. 2 Epoxy resin and burden used to configurator similar materials

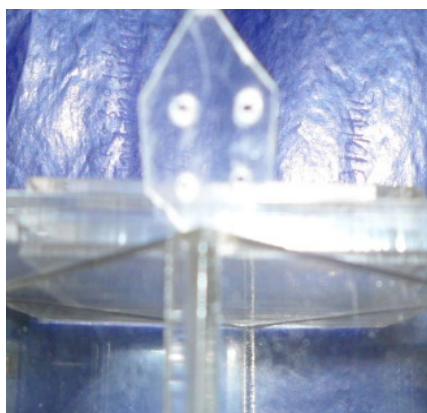


Fig. 3 3D fractures - mica sheet

semi-rigid products, with a good pressure impact. It was transparent yellow liquid, suitable for the manufacture of good toughness and mechanical strength of the shell. This formulation made full use of the brittle and strength of A and B respectively. The two kinds of resins were mixed evenly according to a certain mass ratio. Meanwhile, a good brittle rock specimen was made under the accelerating curing action by the curing agent and accelerator.

In order to improve the tensile and compressive strength ratio of the material, a variety of proportioning tests were carried out.

C material was a kind of medium temperature curing epoxy resin system, with low viscosity, stable performance at room temperature and so on. The appearance was white transparent liquid. It had the characteristics of good brittleness and high strength. The system's activity was adjusted by different curing agent. The resin materials were usually harmless when using in the specified safety measures. The curing agent and accelerator had a pungent smelling, so it was necessary to maintain good ventilation of the experimental site.

2.2 The mechanical properties test of resin materials

Mechanical parameters such as compressive strength, tensile strength were mainly obtained through the uniaxial compression test and splitting tensile test. The trial bond force was got by the related conversion formula.

The test specimens were subjected to uniaxial compression by displacement loading method. The displacement loading rate was 0.03 mm/min, and the Brazil split test was carried out with the same loading rate (0.03 mm/min) until the failure. A variety of experiments were carried out for each scheme, and the optimal tension and compression ratio of these two schemes were shown on Tables 1-2.

Table 1 Physical and mechanical parameters of first scheme

Unsaturated resin AB mixed test	Compressive strength (MPa)	Tensile strength (MPa)	Tension and compression ratio
5:1	83.79	16.1	5.20

Table 2 Physical and mechanical parameters for second scheme

Density (g/cm ³)	Elastic modulus (GPa)	Compressive strength (MPa)	Tensile strength (MPa)	Brittleness degree	Cohesion (MPa)	Internal friction angle (°)	Poisson ratio
2.6	6.5	135	21	6.4	26.5	47.5	0.25

2.3 Making method and material selection of 3-D fracture

The making methods of 3D fractures mainly included the pre - embedding slice method, the slice drawing method, the cutting method and the bending pre - splitting method. The catalyst and the method of controlling the forming temperature were needed, when making the random distribution of the resin samples. The method of pre embedding in the model material was usually used to simulate the internal closed fracture of the sample. The resin material with simulated internal crack had the characteristics of convenient material drawing and small bond strength between the resins. The thin sheet included the metal (steel, iron) sheet, polyethylene sheet and Mica sheet. The material used in this paper was a kind of thin mica sheet, which thickness was 0.1 mm, width was 1.5 mm, length was 2 mm, and the shape is ellipse. The elliptical thin mica sheet was convenient for the positioning of the three-dimensional fracture and more close to the crack in the rock mass, as shown in Fig. 3.

2.4 Fracture of the preset program

In order to compare with the results of previous experiments, a new type of mold with good transparency, size of 70 mm (length) × 70 mm (width) × 140 mm (height), was adopted. As shown in Fig. 4, the mold was composed of 4 pieces of organic glass plate and 1 bases. They were sealed with organic silicone insulation. The good transparency of the mold made it possible to directly observe the specimen curing process in order to select the appropriate time pouring layered. The base and the organic glass plate were separated when the specimen in the mold cured and reached the certain strength. Before pouring, the inner wall was coated with release agent. Only need a little force applied, the specimen could be easily separated from the organic glass plate. Mold

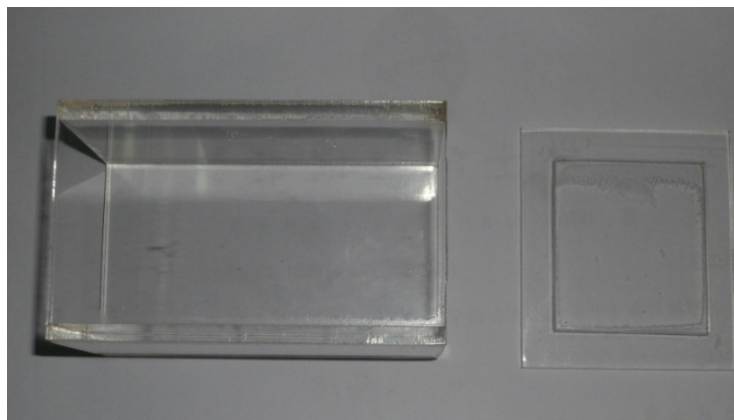


Fig. 4 New improved mold

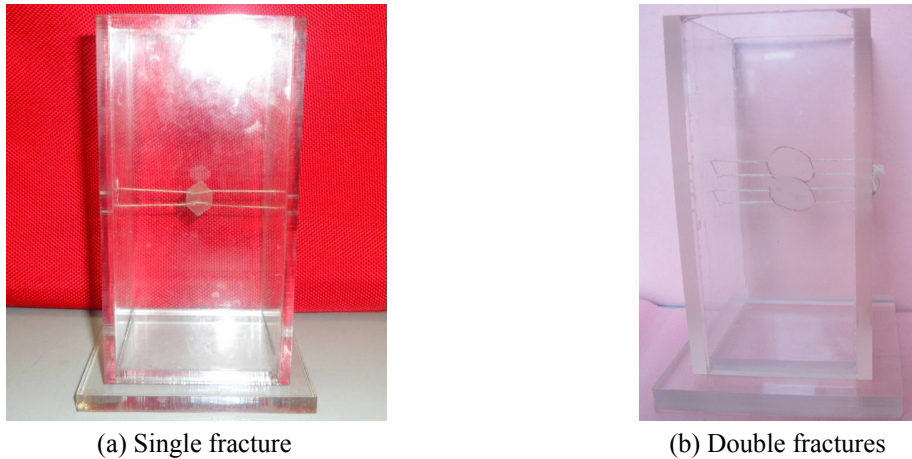


Fig. 5 Specimens containing 3D single and double fractures

could achieve recycling. On both sides of the plate surface of the drill different position around the hole, through the soft thread pulling and fixing to form the different angles, different types of fracture combination. The mold can be used to make three dimensional crack specimens with different number and different stagger distance. Three-dimensional fracture needed pouring material, to minister in the first in the mold positioning and define the fracture plane and the horizontal plane angle for 3D fracture angle. Three dimensional fracture specimens with different angles was fabricated through the developed mold and the mold could also prefabricate different number of three-dimensional fracture specimens, such as double cracks, three cracks, four cracks and other three-dimensional crack specimen. It could also be prefabricated longitudinal type, internal fault type, the top type of the three-dimensional fractures in the specimens. Two molds with single and double fractures were shown on Fig. 5.

3. Test results analysis

3.1 Containing single internal crack specimen failure process under uniaxial load

In order to compare with the previous experimental results, the size of the specimen was 70 mm (length) \times 70 mm (width) \times 140 mm (height). The three-dimensional crack size was that the thickness was 1 mm, the width was 10 mm, and the length was about 15 mm. This section introduced a single fracture specimen with a dip angle of 45 degrees. The fracture was in the middle of the specimen.

This paper selected two experimental results of the program with a relatively high tension and compression ratio. The stress-strain curve (Fig. 6) had four deformation segments (crack compaction, elastic deformation, crack growth and convergence stage, crack acceleration expansion). The crack growth characteristic of single crack specimen was shown in Fig. 7.

- (1) The AB segment was the initial compaction stage. The stress and strain curve was a downward concave nonlinear line. The slope of the stress-strain curve was smaller than the whole specimen, mainly due to the low stiffness of the prefabricated cracks.

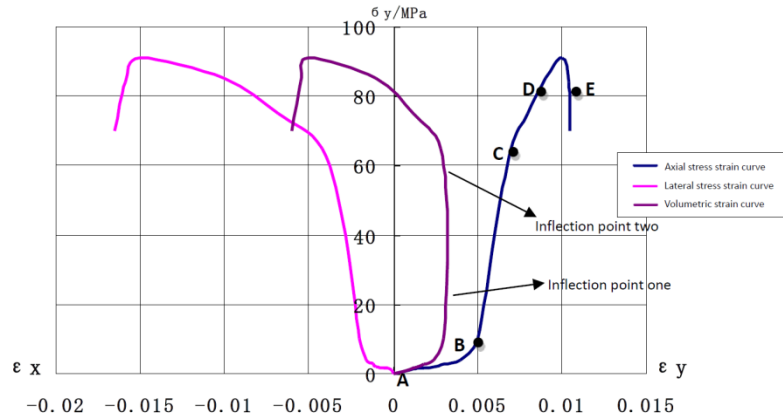


Fig. 6 Stress-strain curve of specimen's failure process

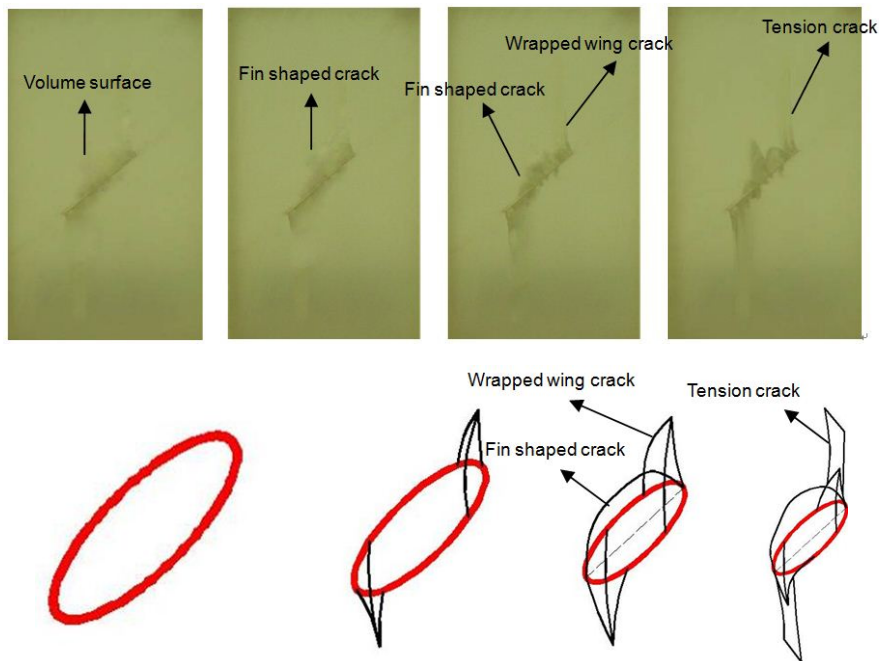


Fig. 7 Propagation process under uniaxial compression for sample containing single fracture

- (2) The BC segment was the elastic deformation stage. The stress increased from 10% to 66% of the peak strength. The axial stress and the axial strain increased linearly. The first inflection point of the volume strain appeared in 23% of the compressive strength.
- (3) Meantime, the new cracks in prefabricated crack long shaft tip initiation were observed. Then, the lower end of the prefabricated crack was formed by a macroscopic parcel surface which was composed of a wrapped wing crack. When the stress reached 60% of the peak value, the volume strain curve had second turning points and there were some new secondary crack growth in the pre-fabricated crack. At the same time, local material

cracking led to the crackling sound generated

- (4) The CD segment was the crack growth and convergence stage. The stress increased from 66% to 88% of the peak strength. The stress and strain curve deviated from the linear downward curve and the curve slope gradually decreased. Wrapped wing cracks were expanded in the form of a curved surface, and extended along the crack edge to the center of the specimen. The new crack extended along the direction of the loading force. Petal type crack from the ends of the pre-existing cracks along the long axis of the end edge parts gradually extended. At the same time, the kink fin shaped fracture surfaced in the middle of the preset crack initiation.
- (5) The DE segment was the entire specimen instability stage. The stress of this stage was from 88% of the peak strength to the failure of the specimen. The formation of the macroscopic rupture zone was observed in the pre-fabricated crack propagation. The whole frame of the specimens were destroyed. With continued loading, the vertical tension crack formed the macroscopic fracture surface and it eventually split the specimen. It presented the brittle cleavage failure.

The stress - strain curves and the four stages of the deformation and rupture process were shown in Fig. 6, which showed that the mechanical properties of the material were very close to the performance of the rock specimens, including the capacity expansion.

3.2 Failure process of double fractures group specimen under biaxial loading condition

This section presented the experimental results of the specimen with double fractures specimen under biaxial stress. The size of the three dimensional crack was still the thickness of 1 mm, width of 10 mm, the length of 15 mm. The dip angle of each fracture was 45 degrees. The two fractures were arranged in a longitudinal direction, and the positions were in the middle position of the specimen.

Biaxial loading was the stress applied to the specimen in the axial direction and the lateral direction. The value of the lateral stress is 5% of the axial stress. The results show that the failure of the specimen is also experienced in four typical stages (shown in Fig. 8), but it was very different from the single axis. The crack growth characteristic of double crack specimen under biaxial loading is shown in Fig. 9.

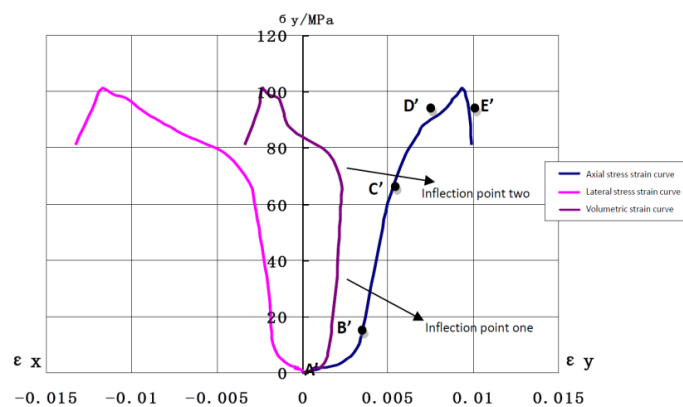


Fig. 8 Stress-strain curve of sample containing double fractures under biaxial compression

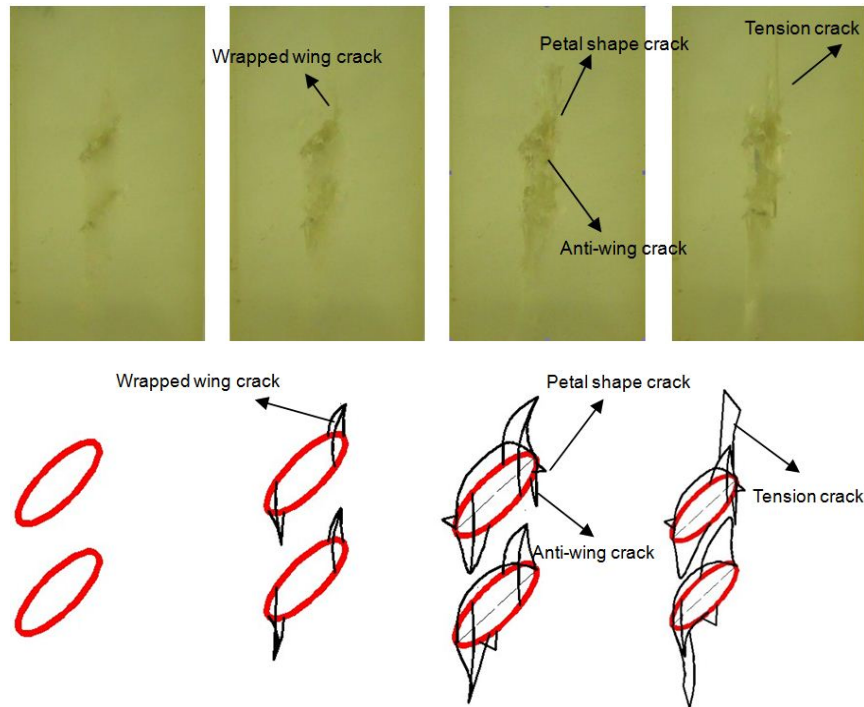


Fig. 9 Propagation process under biaxial loading for sample containing double fracture

- (1) The AB segment was the crack compaction stage. The slope of the curve was larger than the uniaxial compression. The strain was smaller than the strain under the uniaxial compression in this segment.
- (2) The BC segment was the elastic deformation stage. The value of stress was increased from 15% to 62% of the peak strength. The ratio of axial stress and axial strain to fracture specimen was approximately constant. The first inflection point appeared in the volumetric strain curve near the 28% of the strength and it appeared later than the uniaxial compression. At this time, the crack initiation was not observed at the crack tip. As the load continues to increase, the fracture at the fracture tip occurred at 34% of the strength. It was later than the uniaxial load. Along the direction of crack initiation, the wing crack slowly expanded. Wing extension speed was significantly slower than the single axis condition.
- (3) The CD segment was the crack propagation and coalescence stage. The stress was from 62% of the peak strength to 86% of the peak strength. The slope of the stress strain curve was gradually reduced. Wrapped wing cracks were expanded in the front of the prefabricated crack with the layer by layer coverage. The new crack extended along the axial loading direction. Cracks formed in the middle of the fracture surface were complicated by the formation of a complex curved surface. Between the preset two slit crack propagation from the end to the formation of anti-wing crack obviously. While the cracks in the preset petal shape crack extension, but there were no fish fin fractures. At this stage, there were the two slits between the secondary small cracks more than secondary cracks near the original fracture under uniaxial conditions, indicating that under lateral compression and

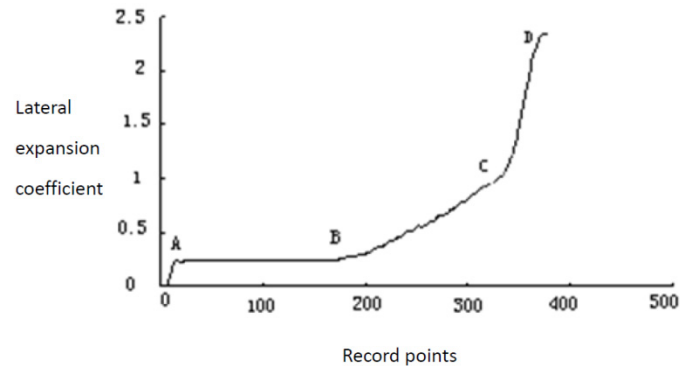


Fig. 10 The lateral expansion coefficient with time

expansion of the wing crack inhibited. Because the stress adjustment effected between the two cracks, the number of the anti-wing crack increased obviously.

- (4) The DE segment was the overall instability stage, with the stress increasing from 86% of the peak intensity to the failure of the specimen. The formation of the split band was smaller than the penetration depth in the uniaxial condition. In the unloading process, the crackling sounds were also heard, which was not found in the previous research. It shows that the brittleness of material were better than the previous.

The following analyze and study focused on the capacity expansion characteristics of fractured specimens under compression. The ratio of the transverse strain and the longitudinal strain was defined as the lateral expansion coefficient.

The Fig. 10 showed the lateral expansion coefficient variation with time. The segment of the OA, AB, BC, CD in Fig. 10 corresponded to the segment of the AB, BC, CD, DE in Fig. 8. The coefficient increased linearly with time in the OA segment. The coefficient increased linearly with time in OA, and the coefficient was basically maintained at a constant rate of about 0.25 in the AB segment, BC segment of the coefficient showed a linear growth, which was the coefficient could reach about 1. When the CD segment was reached, the coefficient was further increased significantly. Finally, the coefficient could reach about 2.5. The brittleness of new materials was obvious and a lot of new cracks generated. The expansion phenomenon was very significant.

4. Conclusions

The brittle transparent material with three-dimensional fractures were made and the fracture propagation experiments were carried out.

- New transparent and brittle materials were developed. Different types and number of three dimensional fractures making methods were established. The brittleness of the material was similar with the rock. The tension and compression ratio could reach above 1/6 at the normal temperature. Material properties were stable and easy to make.
- The failure mechanism and strength characteristics of the specimen containing three dimensional single fracture under uniaxial loading were studied. The four deformation stage of rock specimen included: the initial compaction stage, the elastic deformation stage,

the crack growth and convergence stage and the entire specimen instability stage. The wing crack and other secondary crack under three dimensional crack condition were different from the two-dimensional condition.

- The failure mechanism and strength characteristics of the specimen containing three dimensional double fractures under biaxial loading were studied. It was similar with the uniaxial compression. They all had the four deformation stage. But the fracture growth rates were slower and the initial stress of each stage was higher than the uniaxial compression. Compared with single fracture, the anti-wing crack generated between the two fractures and the expansion of the anti-wing crack resulted in the overlap of the rock bridge.
- The expansion characteristics of the fractured specimens were obvious. Many new cracks generated after compression. The lateral expansion coefficient could up to 2. It was more obvious than the previous research. The previous experiments never obtained this result.

References

- Beygi, M.H.A. (2013), "The effect of water to cement ratio on fracture parameters and brittleness of self-compacting concrete", *Mater. Des.*, **50**, 267-276.
- Cetisli, F. and Kaman, M.O. (2014), "Numerical analysis of interface crack problem in composite plates jointed with composite patch", *Steel Compos. Struct., Int. J.*, **16**(2), 203-220.
- Cheng, Y.F. (2014), "Recent developments in brittle and quasi-brittle failure assessment of engineering materials by means of local approaches", *Mat. Sci. Eng. R*, **75**, 1-48.
- Luo, X., Ge, H. and Ohashi, M. (2012), "Experimental study on ductile crack initiation in compact section steel columns", *Steel Compos. Struct., Int. J.*, **13**(4), 383-396.
- Morozov, N. and Petrov, Y. (2013), *Dynamics of Fracture*, Springer Science & Business Media, New York, NY, USA.
- Mostafavi, M. (2013), "Three-dimensional crack observation, quantification and simulation in a quasi-brittle material", *Acta Mater.*, **61**(16), 6276-6289.
- Ramamurthy, T. (2001), "Shear strength response of some geological materials in triaxial compression", *Int. J. Rock Mech. Min. Sci.*, **38**(5), 683-697.
- Sahouryeh, E., Dyskin, A.V. and Germanovich, L.N. (2002), "Crack growth under biaxial compression", *Eng. Fract. Mech.*, **69**(18), 2187-2198.
- Scholtès, L.U.C. and Donzé, F.V. (2012), "Modelling progressive failure in fractured rock masses using a 3D discrete element method", *Int. J. Rock Mech. Min.*, **52**, 18-30.
- Tang, H.D. (2015), "Mechanical behavior of 3d crack growth in transparent rock-like material containing preexisting flaws under compression", *Adv. Mater. Sci. Eng.*, 1-10.
- Tang, C.A., Liang, Z.Z., Zhang, Y.B. and Xu, T. (2005), "Three-dimensional material failure process analysis", *Key Eng. Mater.*, **300**(1), 1196-1201.
- Wang, J., Li, S.C., Li, L.P., Zhu, W., Zhang, Q.Q. and Song, S.G. (2014), "Study on anchorage effect on fractured rock", *Steel Compos. Struct., Int. J.*, **17**(6), 791-801.
- Zhang, Q.B. and Zhao, J. (2013), "Determination of mechanical properties and full-field strain measurements of rock material under dynamic loads", *Int. J. Rock Mech. Min.*, **60**, 423-439.